


New noninvasive measurement method of optics parameters in a storage ring using bunch-by-bunch 3D beam position measurement data

Xingyi Xu 

Shanghai Institute of Applied Physics, Chinese Academy of Sciences, Shanghai 201800, China
and University of Chinese Academy of Sciences, Beijing 100049, China

Yongbin Leng ^{*}, Yimei Zhou, Bo Gao, Ning Zhang, Jian Chen, and Shanshan Cao

Shanghai Advanced Research Institute, Chinese Academy of Sciences, Shanghai 201204, China
and Shanghai Institute of Applied Physics, Chinese Academy of Sciences, Shanghai 201800, China



(Received 8 February 2021; accepted 1 June 2021; published 14 June 2021)

In order to improve machine performance, the optics parameters of the storage ring need to be measured accurately. The commonly used accelerator optics parameters, including momentum compaction factor and dispersion function, are key parameters that reflect the state of the machine. It is difficult to measure them with traditional methods during the user operation run. Based on a high-resolution bunch-by-bunch three-dimensional measurement system, a noninvasive measurement of momentum compaction factor and the dispersion function was performed at the Shanghai synchrotron radiation facility (SSRF). The dispersion function can be obtained purely from the direct observation results of the bunch-by-bunch 3D position, based on the definition of the dispersion function during normal user operation run without perturbing the beam. The theoretical background and experimental results of the method are discussed in this paper. The measurement results are in good agreement with the design values.

DOI: [10.1103/PhysRevAccelBeams.24.062802](https://doi.org/10.1103/PhysRevAccelBeams.24.062802)

I. INTRODUCTION

Precise knowledge of key accelerator parameters are important for the analysis of many beam dynamics measurements and user experiments, as well as to tweak the related model of the accelerator [1]. Among others, the momentum compaction factor and the dispersion function are important beam optics parameters of the accelerator. The momentum compaction factor is a parameter related to the properties of the magnetic guide field, and it is a core parameter in the description of synchrotron, i.e., energy oscillation. The dispersion function is a parameter that reflects the deviation of the electron beam orbit caused by a momentum shift. The distribution of the dispersion function can be used to analyze the orbit focusing performance, and the optimization of the dispersion function can ensure the stability of the beam orbit.

A noninvasive measurement method refers to the measurement of parameters locally, without affecting the daily operation of the facility. Because it does not require special machine study time, the operating efficiency of the

synchrotron facility can be improved. Therefore, noninvasive measurements of machine parameters have always been the direction that accelerator BI (beam instrument) scholars are trying to explore [2–5].

The momentum compaction factor and dispersion function cannot be measured noninvasive without disturbing the ordinary light supply of the synchrotron radiation facility by conventional means. The reason is, traditional methods to measure these optics parameters require a large variation of the beam energy and orbit, by altering the rf (radio frequency) frequency, which are incompatible with the daily operation of a synchrotron radiation facility [6–9].

In this paper we present a new noninvasive method to measure the momentum compaction factor and dispersion function, based on high-resolution, bunch-by-bunch, three-dimensional beam position monitoring (BPM) system. The top-up operation mode is applied at SSRF, which means that injection is very frequent. By applying the single bunch refilled charge extracting algorithm, a three-dimensional position trajectory, having a large oscillation amplitude for the injected bunch, can be retrieved from the captured transient data of the injection. A fit of the measured longitudinal bunch position results in a trace showing the longitudinal bunch oscillations, revealing a precise value of the longitudinal tune and momentum compaction factor. An analysis of the correlation between the measured longitudinal and horizontal bunch position gives an information about the dispersion function. All this can be

^{*}lengyongbin@sinap.ac.cn

Published by the American Physical Society under the terms of the *Creative Commons Attribution 4.0 International license*. Further distribution of this work must maintain attribution to the author(s) and the published article's title, journal citation, and DOI.

TABLE I. Parameters of SSRF.

Parameter	Value
Energy (E)	3.5 GeV
Current (I_0)	220 mA
rf frequency (f_{rf})	499.654 MHz
rf cavity voltage (V_{rf})	4.5 MV
Buckets (h)	720
Revolution frequency (f_o)	694 kHz
Bunch length (σ)	18 ps

performed during normal user operation run without disturbing the beam, which makes its method very attractive for a synchrotron light user facility.

In recent years, the bunch-by-bunch, three-dimensional beam position measurement system has been successfully deployed at the SSRF [10–16]. The facility is a third generation synchrotron radiation light source. It is composed of a group of accelerators: a 150 MeV linear accelerator, a 180 m-long 3.5 GeV booster, and a 432 m long 3.5 GeV storage ring. The machine runs routinely in top-up mode. Four bunch trains, each has 125 consecutive bunches, are evenly spread in the 720 buckets in the storage ring. The relevant parameters of the machine are listed in Table I.

A three-dimensional, bunch-by-bunch beam position measurement refers to the simultaneous measurement of the transverse position, longitudinal phase, and charge of any bunches in the storage ring. Based on this system, small changes in the behavior of the bunches can be detected, which is relevant to study the beam dynamics of the accelerator, but puts high demands on the resolution of the measurement system. We improved the performance of this bunch-by-bunch measurement system, the resolution of longitudinal phase is better than 0.2 ps, the resolution of transverse position is better than 10 μm and the charge resolution is 0.3%. The system meets the measurement requirements.

The “top-up” operation mode requires frequent injection to maintain a constant high current. This top-up injection process is a perturbation to the storage ring, which will kick the beam far away from the equilibrium point. The refilled bunch contains the stored charge and refilled charge. The signal collected by the beam position monitors is a combination of the stored charge and refilled charge. During the injection process, the three-dimensional movement of the newly refilled charge carries different information from the three-dimensional movement of the stored charge. Only the longitudinal movement of the newly refilled charge gives relevant information for the accurate extraction of the longitudinal oscillation frequency. In order to study it, the refilled charge signal needs to be extracted out and studied separately. Therefore, based on the response function and the bunch-by-bunch measurement

technique, a set of refilled charge signal extracting algorithm was developed. Using this algorithm, the refilled charge signal is extracted the original mixed refilled bunch signal, and the three-dimensional position and charge of the refilled charge portion of the bunch are further analyzed. The transient behavior of the refilled charge portion is used to measure the beam optics parameters without disturbance of the stored beam.

The basic principle of the beam position measurement system is explained in Sec. II. The measurement system is shown in Sec. III. In Sec. IV, we present the measurement results of the noninvasive beam optics parameter measurement. In Sec. V, we analyze the performance of this noninvasive optics parameters measurement method, including applicable conditions and uncertainty. In order to further verify the feasibility of the measurement method, a proof experiment is presented in Sec. VI. Section VII provides a short summary.

II. THEORETICAL BACKGROUND

Particles with different momenta in a storage ring will follow different closed orbit trajectories of different path lengths. The momentum compaction factor α_c is defined as:

$$\alpha_c = \frac{\Delta L/L}{\Delta p/p}. \quad (1)$$

where L is the length of the closed orbit and p is the momentum of the particle [17,18].

The period of the particle revolution τ depends on the momentum deviation, due to the change of the closed orbit length and the change of the particle velocity, as:

$$\frac{\Delta\tau}{\tau} = \left(\frac{1}{\gamma^2} - \alpha_c\right) \frac{\Delta p}{p} = \eta_c \frac{\Delta p}{p}, \quad (2)$$

where γ is the Lorentz factor and η_c is the slip factor. For high energy electron storage rings, the velocity change due to a change of momentum is negligible and $\eta_c = -\alpha_c$.

For the storage ring:

$$\tau = \frac{h}{f_{\text{rf}}}, \quad (3)$$

where h is the harmonic number of available rf buckets of the storage ring and f_{rf} is the frequency of the rf cavities. Equation (2) can be written as:

$$\frac{\Delta f_{\text{rf}}}{f_{\text{rf}}} = -\alpha_c \frac{\Delta p}{p} = -\alpha_c \frac{\Delta E}{E}. \quad (4)$$

where E is particle energy.

Therefore, in order to precisely measure the momentum compaction factor, conventional methods require to greatly

alter the beam energy, and measure the effects in energy using methods, like the depolarization resonance [19].

A different method to obtain the momentum compaction factor, without affecting the daily user operation, utilizes the synchrotron damping process of the energy oscillations. The energy oscillation equation is expressed as:

$$\frac{d\varepsilon}{dt} = \frac{eV_{\text{rf}} - U_{\text{rad}}}{\tau}. \quad (5)$$

where ε is deviation energy and U_{rad} is energy lost by synchrotron radiation. For small deviations from the nominal beam energy (particle energy is close to the energy of the synchrotron particle), the longitudinal motion of the particle appears as a typical synchrotron damping oscillation [17,18], in the form of:

$$z_d = z_m \sin\left(\sqrt{\Omega^2 - \lambda_s^2}t + \varphi_0\right)e^{-\lambda_s t}. \quad (6)$$

where the reciprocal of λ_s is the synchrotron damping time. φ_0 is the arrival time of the bunch. The synchrotron frequency is $\Omega = 2\pi\nu_s$ and z_m is the oscillation amplitude. The synchrotron tune ν_s is determined by the following set of accelerator parameters:

$$\nu_s = \frac{2\pi E}{\alpha_c e h V_{\text{rf}} [1 - (U_{\text{rad}}/eV_{\text{rf}})^2]^{1/2}}. \quad (7)$$

Due to $U_{\text{rad}} \ll eV_{\text{rf}}$, Eq. (7) can be simplified as:

$$\alpha_c = \frac{2\pi E \nu_s^2}{e h V_{\text{rf}}}. \quad (8)$$

Except for the synchrotron tune, the parameters on the right side of Eq. (8) can be directly obtained during the daily operation of the facility. The actual synchrotron tune is the only free, to be measured parameter for completing the noninvasive momentum compaction factor measurement. We plan to measure the synchrotron tune during the frequent injection process in the “top-up” operation mode.

In the electron storage ring, the dispersion function [$\eta(s)$] is a parameter that reflects the deviation of the electron orbit caused by a shift of the beam momentum, which can be measured by altering the rf frequency, resulting in a change of the horizontal beam orbit. According to the definition, the horizontal shift of the electron beam orbit can be expressed as:

$$\Delta x = \eta(s) \frac{\Delta p}{p}. \quad (9)$$

According to the definition of momentum compaction factor [Eq. (4)], this leads to:

$$\eta(s) = -\alpha_c \frac{\Delta x}{\Delta f_{\text{rf}}/f_{\text{rf}}}. \quad (10)$$

Therefore, in order to precisely measure the dispersion function, it is necessary to simultaneously measure the horizontal beam orbit and the rf frequency, as that frequency needs to be varied largely when applying conventional methods.

According to the basic definition [Eq. (2) and Eq. (9)], the following equation can be derived:

$$\eta(s) = -\alpha_c \frac{\Delta x}{\Delta \tau/\tau}. \quad (11)$$

Based on Eq. (8) and Eq. (11), a noninvasive measurement method of the momentum compaction factor and dispersion function will be introduced in this paper without “artificially” changing particle energy and rf frequency.

III. THE MEASUREMENT SYSTEM

Based on the 3D bunch-by-bunch position measurement system, a hardware module which consists of a broadband oscilloscope as the core and a software module with the refilled charge extraction method as the core are used for noninvasive measurement of the beam optics parameters. The system framework is shown in Fig. 1.

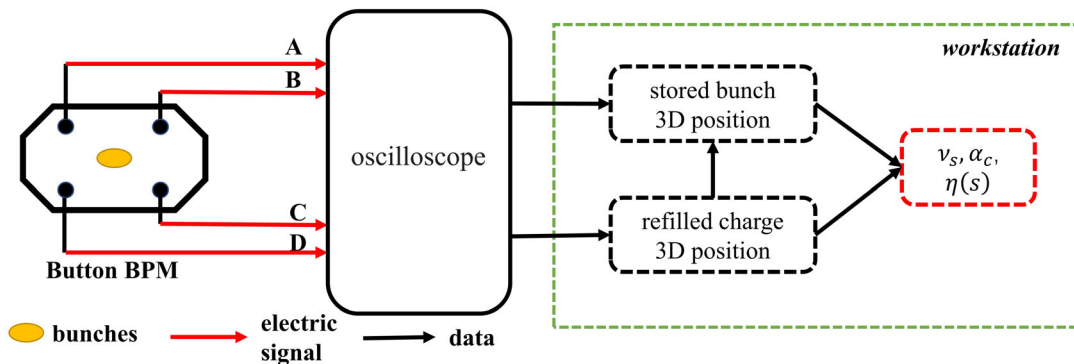


FIG. 1. The BPM measurement setup of the beam optics parameter measurement system.

In this system, button beam position monitors (BPMs) are used as bunch signal source. There are 140 BPMs, distributed in 20 cells, along the circumference of the storage ring of the SSRF. A broadband oscilloscope with 25 GS/s maximum sampling rate and 10 GHz maximum analog bandwidth was chosen to record the signals from the four button electrodes of the BPMs.

The data processing was performed in a workstation computer. A software module was used to extract the three-dimensional bunch position from the measured signal waveforms of the oscilloscope. In addition, the function of the software module also includes the extracting of the bunch signal related to that of a refilled bunch charge, allowing to subtract the stored charge portion from the refilled bunch to enable the study of instability phenomena in a stable operating regime. Finally, the three-dimensional position of the refilled portion of the bunch and the three-dimensional position of the stored bunch are used to further evaluate the beam optics parameters. Among them, the extracting of the refilled charge signal and the extraction of the three-dimensional position are not in the focus of this paper, and are only briefly discussed in this section.

The four electrode signals generated by a bunch passing through the BPM pickup is acquired by a 4-channel broadband oscilloscope, and are short pulse waveforms of about 0.5 ns duration, and as consequence even with a high sampling rate the number of relevant sample points of the pulse signal is low. Each bunch appears periodically at each BPM in the storage ring with a rate defined by the revolution frequency. Since there is no synchronicity between the sampling clock of the oscilloscope and the rf frequency of the accelerator, the signals acquired by the oscilloscope have a different sampling phase with regard to BPM pulse signals for each bunch passage of the BPM pickup. The picture of the entire waveform of the bunch response signal of one BPM pickup electrode, i.e., the reference response signal in Fig. 2, was generated by combining all bunch response signals of several thousand consecutive turns.

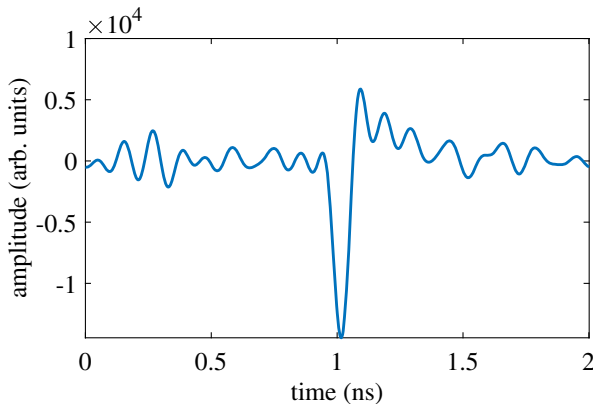


FIG. 2. Bunch signal response waveform of a BPM electrode, acquired with 10 GHz bandwidth.

The relative signal amplitude and relative longitudinal phase of each bunch, at every turn was obtained comparing the actual signal of each bunch, turn-by-turn, with the reference response signal.

The transverse beam position (x, y) and the bunch charge (Q) for a specific bunch are computed as follows:

$$\begin{aligned} x(i) &= k_x \cdot \frac{A(i) - B(i) - C(i) + D(i)}{A(i) + B(i) + C(i) + D(i)} \\ y(i) &= k_y \cdot \frac{A(i) + B(i) - C(i) - D(i)}{A(i) + B(i) + C(i) + D(i)} \\ Q(i) &= k_q \cdot (A(i) + B(i) + C(i) + D(i)). \end{aligned} \quad (12)$$

with k_x , k_y , and k_q being constants, given by the BPM pickup and the gain of the signal processing chain. $A(i)$, $B(i)$, $C(i)$, $D(i)$ are the relative signal amplitudes of the four BPM electrodes A, B, C, and D respectively, at the i th turn.

IV. EXPERIMENTS RESULTS

The noninvasive measurement method is applied to measure momentum compaction factor and dispersion function at the SSRF storage ring. The experiment does not need any special configuration of the machine, the data was acquired unnoticed during daily operations (top-up mode). The “top-up” operation mode requires frequent injection to maintain a constant high current. Both, the beam data collected during the injection transient, and the beam data collected during the stable state were used for the analysis of beam optics parameters. The reason to select the injection transients, in particular the refilled charge portion of the refilled bunches, is simply the fact that those undergo a strong, but of course damped synchrotron oscillation excitation. The capture of injection transient process appeared to be a difficult task due to the small amount of refilled charge. The injection event cannot be observed directly, however, the range in signal amplitude after the injection is quite large among the injected data. In the following, the stored bunches exhibit significant transverse oscillation, while the refilled charge has a large longitudinal, while the refilled charge portion has large longitudinal oscillations. Therefore, the amplitude difference of the refilled charge is obviously greater than that of the other stored bunches. Based on this, a software trigger threshold can be set up, from which we can select the injected data group and mark the refilled bunches [16]. Typical results plotted in this section were processed by using the data recorded on July 25, 2020 unless otherwise noted.

A. Momentum compaction factor

The momentum compaction factor can be calculated according to Eq. (8). In order to accurately calculate the

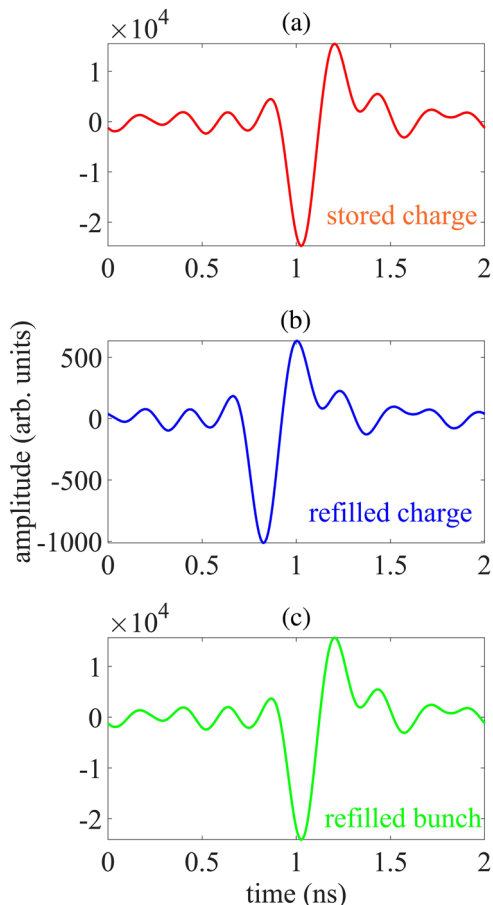


FIG. 3. Signal waveform of, (a) the stored charge, (b) the refilled charge, and (c) the refilled bunch charge as sum of (a) and (b).

momentum compaction factor, an accurate real-time measurement of the synchrotron tune is crucial. During the injection process, due to the mismatch between the injector and the storage ring, the refilled charge typically undergoes a damped synchrotron oscillation. In order to obtain the synchrotron tune, it is necessary to extract the refilled charge signal from the acquired BPM signal, containing a mix of stored and refilled charge in the bunch.

During each injection process, typically 3 to 5 buckets of the SSRF storage ring are refilled, each stored bunch charge is merged with the refilled charge and represent a refilled bunch.

Figure 3 shows the typical signal waveform of, (a) the stored charge, (b) the refilled charge, and (c) the refilled bunch charge as sum of (a) and (b).

All stored bunches, several hundred in typical runs, follow basically the same transverse and longitudinal motion pattern. Therefore, any stored bunch signal is representative as signal of the stored charge, and valid for the refilled charge signal extraction algorithm. In order

TABLE II. Beam parameters of the storage ring.

Parameter	Value
Stored charge (Q_s)	582 pC
Refilled charge (Q_r)	21.0 pC
Oscillation amplitude (z_m)	603.7 ± 7 ps
Refilled charge arrived time (φ_0)	3.07 ± 0.01 rad
Synchrotron damping time (T_r)	2.82 ± 0.05 ms
Synchrotron tune (ν_s)	0.007308 ± 0.000002

to reduce the measurement error, we chose a sufficient bucket distance N , typically $N = 20$, of stored bunches separated from the refilled bunch as our reference stored charge signal. The signal of the refill charge was obtained by subtracting the signal of the stored charge from the signal of the refilled bunch.

The turn-by-turn longitudinal phase of the refilled charge was extracted from the refilled bunch signal using the bunch-by-bunch three-dimensional measurement algorithm. A mathematical model for the evolution of the longitudinal phase oscillations was used to fit the parameters in Eq. (6). Table II lists the beam parameters used for the fitting algorithm, and Fig. 4 compares the refilled charge phase evolution extracted from the measurement with the fit.

According to Eq. (8), the current momentum compaction factor of SSRF is 4.078×10^{-4} .

B. Dispersion function

The dispersion function can be calculated according to Eq. (11). Even during daily operations of the synchrotron radiation facility, the revolution period τ of the beam will shift relative to the set value due to an instability. The shift is very small, approximately $1e-6$ of the revolution time. This shift of the revolution period will be coupled to the orbit. Therefore, by accurately measuring both effects, the value of the dispersion function was obtained. Based on the 3D bunch-by-bunch measurement system, the

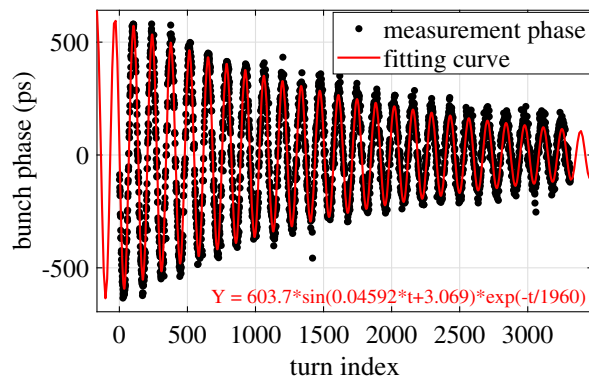


FIG. 4. The measured refilled charge phase and the fitting curve. Black dot line: the measured refilled charge phase; red solid line: fitting trace of the refilled charge phase.

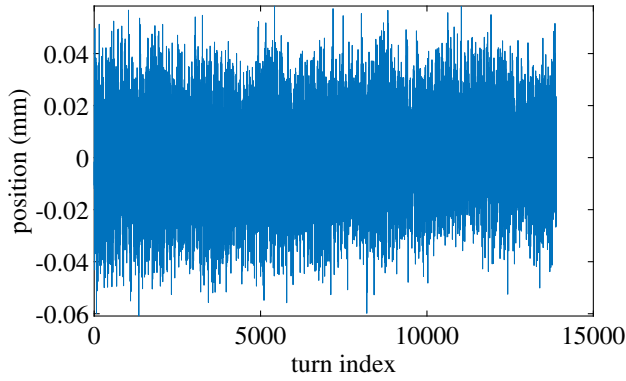


FIG. 5. The measured turn-by-turn horizontal position $[x(i)]$ vs. turn i for a common bunch.

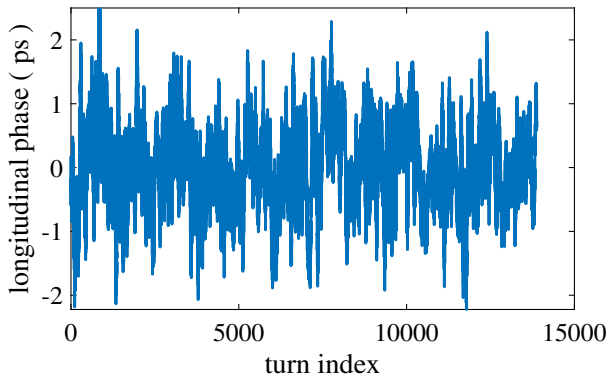


FIG. 6. The measured turn-by-turn longitudinal phase $[\varphi(i)]$ of a common bunch.

horizontal beam position $[x(i)]$, and the longitudinal phase $[\varphi(i)]$ of a bunch was accurately measured, as shown in Fig. 5 and Fig. 6.

The horizontal bunch position of the i th turn $[x(i)]$ is a linear superposition of four components:

$$x(i) = x_o + \Delta x(i) + x_\beta(i) + \sum_n x_n(i). \quad (13)$$

where x_o is the reference orbit. $\Delta x(i)$ is the orbit shift caused by the coupling to the shift of the revolution period. $x_\beta(i)$ is related to betatron oscillation. $x_n(i)$ reflects all the various noise contributions in the orbit measurement. Only $\Delta x(i)$, the orbit shift related to the shift of the revolution period, is relevant for the dispersion function. Typically, the other components are small, however, to improve the accuracy it is valuable to minimize their contribution.

The spectral analysis results of the turn-by-turn horizontal position and longitudinal phase of a common bunch are shown in Fig. 7. The high frequency part of the frequency spectrum of the horizontal position has peaks caused by betatron oscillation and its higher harmonics. In addition, both spectra have a uniformly distributed noise

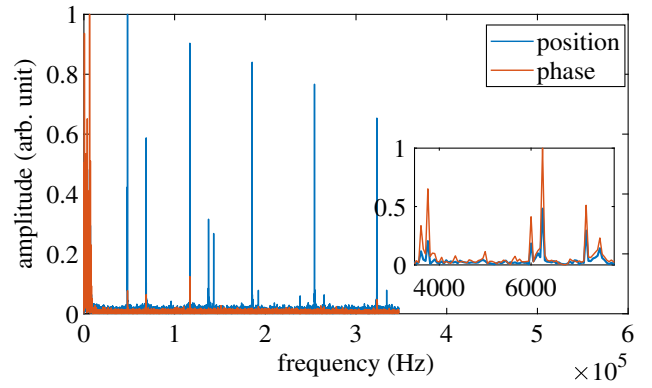


FIG. 7. The spectral analysis results of the turn-by-turn horizontal position and longitudinal phase of a common bunch. Blue solid line: the spectral of turn-by-turn horizontal position; red solid line: the spectral of turn-by-turn longitudinal phase. The small figure on the right is the close-up of 4000 Hz–8000 Hz.

floor generated by the measurement system. In the low frequency part, the two frequency spectra coincide (see the zoomed plot inside Fig. 7). A low-pass filter frequency discrimination was used to suppress the higher harmonics, in this way the coupling of the shift of the revolution period ($\Delta\tau$) and the orbit shift (Δx) can be retained.

$$\Delta\tau(i)/\tau = \frac{\varphi(i) - \varphi(i-1)}{\tau}, \quad (14)$$

where $\Delta\tau(i)$ is the shift of the period of the bunch revolution of the i th turn. $\varphi(i)$ is the longitudinal phase in the i th turn. τ is the revolution time (period) of the bunch. According to Eq. (14), the relative shift of the period was obtained by differentiating the turn-by-turn longitudinal phase.

The correlation between the normalized shift of the revolution period, $\Delta\tau(i)/\tau$, and the orbit shift, Δx , is linear, as shown for several thousand turns in Fig. 8. Following

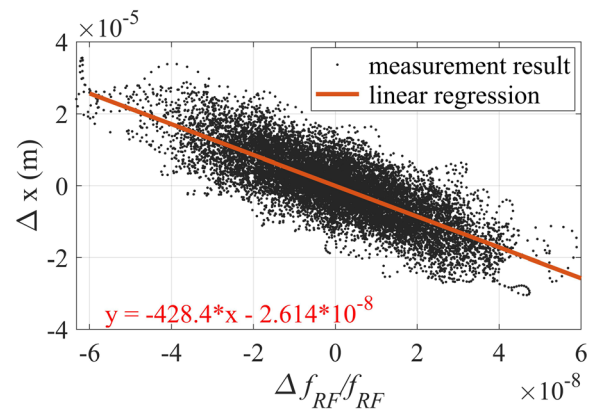


FIG. 8. The correlation between the normalized shift of the revolution period, $\Delta\tau/\tau$, and the orbit shift, Δx , is linear. Black dots: measured results of 14000 turns; red solid line: linear regression.

Eq. (11), the value of the dispersion function at this measurement location was determined to be 0.1747 m.

V. PERFORMANCE EVALUATION

The following will analyze the performance of this noninvasive optics parameters measurement method, including applicable conditions and uncertainty.

The measurement method has no special requirements for the beam state and can be carried out in the daily operation of the synchrotron radiation facility. As of the sufficient high refresh rate of the parameter calculation, the measurement system is able to detect changes of the storage ring optics parameters in real-time. The refresh rate of the momentum compaction factor depends on the filling frequency of the top-up mode (approximately once every 5 minutes for SSRF), and the refresh rate of the dispersion function is not limited (approximately 10 Hz). Since there are no special applicable conditions, this method has the potential to be applied in many other 3rd generation synchrotron light sources. However, the momentum compaction factor is calculated using the signal collected during the injection transient. In the “top-off” mode (infrequent injection), the refresh rate is typically rather low. In addition, the bunch-by-bunch three-dimensional measurement system is the basis of this method.

The uncertainty of the momentum compaction factor and dispersion function measurement was analyzed. The design value of the momentum compaction factor is 4.2×10^{-4} in SSRF. It is consistent with the experimental results (4.078×10^{-4}). The measurement uncertainty mainly comes from the fitting of the synchrotron tune (shown in Fig. 4). The confidence interval for the synchrotron tune is $[7.307 \times 10^{-3}, 7.310 \times 10^{-3}]$ with 95% confidence bounds. According to Eq. (8), the confidence interval for the momentum compaction factor is $[4.077 \times 10^{-4}, 4.080 \times 10^{-4}]$.

In the above analysis, only the three-dimensional position of a single bunch is used to calculate the dispersion

function value. In fact, more than 400 bunches in the storage ring can be used to calculate the dispersion function independently at the same time (shown in Fig. 9).

Using one standard deviation as definition of the uncertainty of a single independent measurement, we find a uncertainty value of 0.0066 m for the dispersion function measurement (about 3.8%). In the actual measurement, the average value of more than four hundred independent measurement results can be utilized to improve the final measurement value. The processing gain is the square root of 400. Therefore, the relative measurement uncertainty of this dispersion function measurement method is about 0.2%.

VI. PROOF EXPERIMENT

In order to verify performance and robustness of the measurement method, some proof experiments were done in SSRF. In the first experiment, 3 bunches were injected into a previously empty storage ring. These injected bunches have large longitudinal and transverse oscillation during the injection transient which can be used to measure the momentum compaction factor and dispersion function. In the second experiment, the dispersion function values at the seven different BPMs position of cell 19th were measured during daily operation (stable beam). The applicability of the measurement method was verified by comparing the measured dispersion function of this cell with the design value.

A. Injection transient with empty storage ring

The results presented in this subsection were processed by using the data recorded on December 3, 2020. The horizontal position and longitudinal phase of the injected bunch were obtained based on the bunch-by-bunch three-dimensional measurement system (shown in Fig. 10). In the same way as described in Sec. IV, a mathematical model

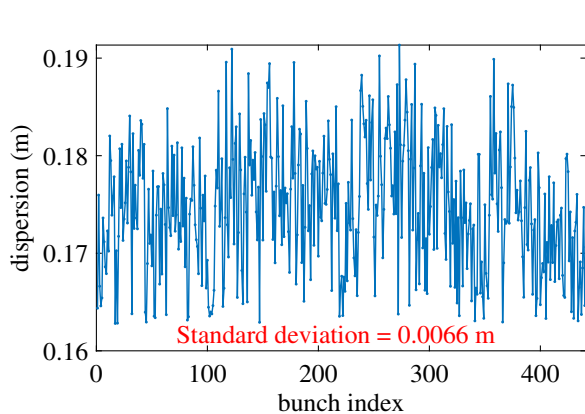


FIG. 9. More than 400 bunches were used to calculate the dispersion function on a basis of independent measurements. The standard deviation of each measurement is 0.0066 m.

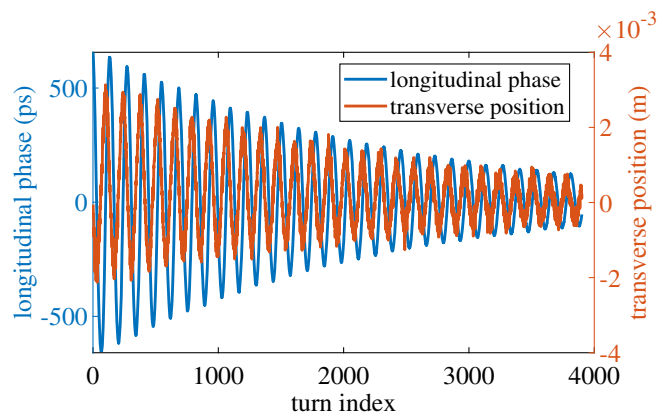


FIG. 10. The measured turn-by-turn horizontal position $[x(i)]$ and longitudinal phase $[\varphi(i)]$ of a refilled bunch. Blue solid line: longitudinal phase; red solid line: horizontal position.

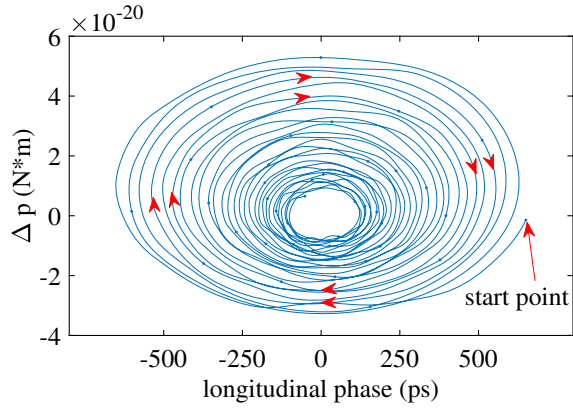


FIG. 11. The evolution in energy phase space of an injected bunch after injection.

was used to fit the evolution of longitudinal phase to acquire the synchrotron tune. The confidence interval for the synchrotron tune is $[7.326 \times 10^{-3}, 7.329 \times 10^{-3}]$ with 95% confidence bounds. Following Eq. (8), the confidence interval for the momentum compaction factor measurement is $[4.098 \times 10^{-4}, 4.101 \times 10^{-4}]$. This result is consistent with that of the previous section.

Combining Eq. (11) and Eq. (14), the following equation can be obtained:

$$\Delta x = \frac{\eta(s)}{-\tau\alpha_c} \frac{d\varphi}{dt}. \quad (15)$$

Where $\varphi(i)$ is the longitudinal phase. From Fig. 10 follows, there is a constant one quarter phase difference between the longitudinal phase and the horizontal position. This result is consistent with the Eq. (15).

According to Eq. (9), the change in particle momentum can be obtained from the horizontal beam position. The measurement result are visualized as phase space diagram,

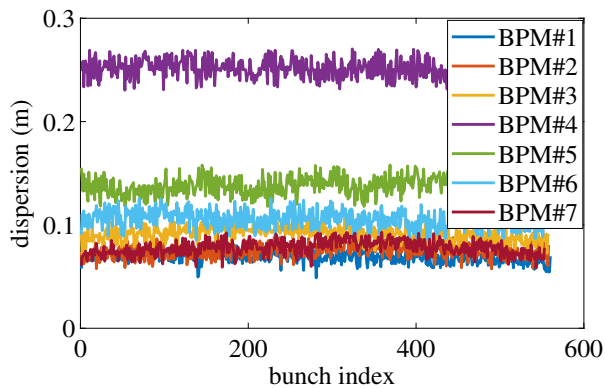


FIG. 12. More than 400 bunches was used to calculate the dispersion function independently. The calculation results of the dispersion function at different locations along the accelerator circumference (at different BPMs) are expressed in different colors.

TABLE III. Dispersion value distribution in a cell.

Position	No. 1	No. 2	No. 3	No. 4	No. 5	No. 6	No. 7
Value (m)	0.0688	0.0749	0.0915	0.2511	0.1379	0.1054	0.0780

and appear as “fish” envelopes. Figure 11 shows the evolution of the trajectory in an energy vs. phase space plot of an injected bunch.

In a similar way the dispersion function at the measurement location was computed from the same set of measurement data. Since the synchrotron oscillation amplitude is dominant, the coupled component for the synchrotron oscillation in the horizontal position is much larger than the effect of the betatron oscillation. The dispersion function measurement was improved by passing the low-pass filtering. Again, the acquired results are consistent with those of the previous section.

B. Dispersion function measurement with a stable beam

The dispersion function ($\eta(s)$) is a function related to the location s along the accelerator circumference(s). The dispersion value reflects the focusing the focusing effect, which changes with regard to the location. The storage ring consists of 20 cells. There are 7 BPMs in each cell. Seven sets of data from seven BPMs are recorded respectively. The dispersion function distribution in a cell is shown in Fig. 12). The results discussed in this subsection were processed by using the data recorded on January 6, 2021.

The average value of more than four hundred independent measurement results (more than 400 bunches) were used to compute the final measurement value, shown in Table III).

The measured result is compared with the parameter design value of SSRF. As Fig. 13 shows, the measured results are in good agreement with the design value.

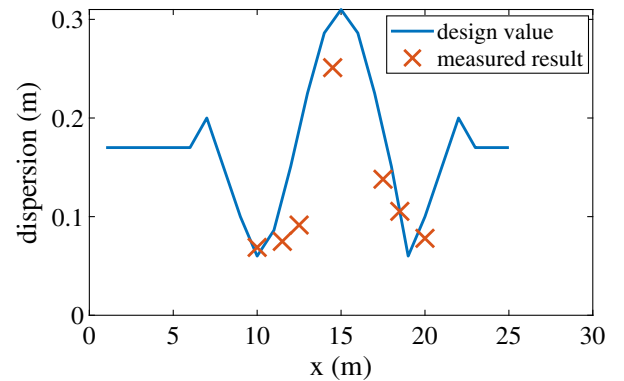


FIG. 13. The dispersion function distribution in a cell of SSRF (No. 19 cell). Blue solid line: design value; red cross: measured value.

VII. CONCLUSION

Commonly used accelerator optics parameters, including momentum compaction factor and dispersion function, are key parameters that reflect the operational status of the machine. This paper describes a new, noninvasive method to measure those parameters utilizing bunch-by-bunch 3D BPM data. The momentum compaction factor that can be obtained relies on the injections. In the top-up mode, the injection is very frequent and the measurement refresh rate is high. In the top-off mode, this method can also be used to obtain the momentum compaction factor. Due to the infrequent injection (usually once every few days), the measurement refresh rate of the momentum compaction factor decreases accordingly. The dispersion function can be obtained purely from the direct observation results of the bunch-by-bunch 3D position based on the definition of the dispersion function which does not depend on the injection frequency.

A series of experiments had confirmed that this noninvasive method is adequate in key optics parameter measurement during daily operation without additional machine study hours. The momentum compaction factor and dispersion function was obtained from the raw BPM data by using bunch-by-bunch measurement algorithm without disturbing the ordinary operation of a light source. Since there is almost no need for special application conditions that only depend on the oscillations caused by injection which is almost inevitable, this method can be widely used in other synchrotron radiation devices.

In addition to real-time monitoring of the machine status during daily operation, this method can analyze the influence of different insertion devices and machine parameter settings on the optics parameters, but also help to optimize the machine setting.

ACKNOWLEDGMENTS

This work was supported by Ten Thousand Talent Program and National Natural Science Foundation of China (No. 11575282) and Ten Thousand Talent Program and Chinese Academy of Sciences Key Technology Talent Program. Thanks to the SSRF Operation Group for their help in the experiment.

-
- [1] J. Schmidt, W. Hillert, M. Schedler, and J.-P. Thiry, Measurement of momentum compaction factor via depolarizing resonances at ELSA, in *Proceedings of IPAC15, Richmond, USA*, International Particle Accelerator Conference (JACoW, Geneva, Switzerland, 2015), pp. 811–813, <https://doi.org/10.18429/JACoW-IPAC2015-MOPHA015>.
- [2] C. Christou *et al.*, In-situ measurement of beam-induced fields in the s-band accelerating structures of the diamond light source linac, in *Proceedings of LINAC2012, Tel-Aviv,*

Israel (2012), <http://accelconf.web.cern.ch/LINAC2012/papers/mopb016.pdf>.

- [3] W. Coosemans and S. Redaelli, In-situ vibration measurements of the ctf2 quadrupoles, in *Proceedings of the 9th European Particle Accelerator Conference, Lucerne, 2004* (EPS-AG, Lucerne, 2004) [<http://accelconf.web.cern.ch/AccelConf/e04/>].
- [4] T. Tanaka, T. Seike, A. Kagamihata, T. Schmidt, A. Anghel, M. Brügger, W. Bulgheroni, B. Jakob, and H. Kitamura, In situ correction of field errors induced by temperature gradient in cryogenic undulators, *Phys. Rev. ST Accel. Beams* **12**, 120702 (2009).
- [5] Z. Chen, Y. Yang, Y. Leng, and R. Yuan, Wakefield measurement using principal component analysis on bunch-by-bunch information during transient state of injection in a storage ring, *Phys. Rev. ST Accel. Beams* **17**, 112803 (2014).
- [6] N. Carmignani, W. D. Nolf, A. Franchi, B. Nash, C. J. Sahle, and L. Torino, Measurements of the momentum compaction factor of the ESRF storage ring, *J. Phys. Conf. Ser.* **1350**, 012023 (2019).
- [7] Mueller, Kalefa, Birkel, Huttel, Perez, and Pont, Momentum compaction factor and nonlinear dispersion at the anka storage ring, in *Proceedings of the 9th European Particle Accelerator Conference, Lucerne, 2004* (EPS-AG, Lucerne, 2004) [<http://accelconf.web.cern.ch/AccelConf/e04/>].
- [8] X. Zhou, Measurement of optics for the SSRF storage ring in commissioning, *Chin. Phys. C* **33**, 78 (2009).
- [9] D. Turner, New methods for dispersion measurement and correction for 12 GeV CEBAF, in *Proc. IPAC 2018, Vancouver, Canada* (JACoW, Vancouver, Canada, 2018), pp. 4882–4884, <https://doi.org/10.18429/JACoW-IPAC2018-THPML094>.
- [10] H. Chen, J. Chen, B. Gao, and Y. Leng, Bunch-by-bunch beam size measurement during injection at Shanghai synchrotron radiation facility, *Nucl. Sci. Tech.* **29**, 79 (2018).
- [11] Y. Yang, Y. Leng, Y. Yan, and N. Zhang, Bunch-by-bunch beam position and charge monitor based on broadband scope in ssrf, in *Proceedings of the 4th International Particle Accelerator Conference, IPAC-2013, Shanghai, China, 2013* (JACoW, Shanghai, China, 2013), p. 595.
- [12] L. Duan, Y. Leng, R. Yuan, and Z. Chen, Injection transient study using a two-frequency bunch length measurement system at the SSRF, *Nucl. Sci. Tech.* **28**, 93 (2017).
- [13] Y. Zhou, H. Chen, S. Cao, and Y. Leng, Bunch-by-bunch longitudinal phase monitor at SSRF, *Nucl. Sci. Tech.* **29**, 113 (2018).
- [14] X. Xu, Y. Leng, and Y. Zhou, Machine learning application in bunch longitudinal phase measurement, in *Proceedings of the 10th International Particle Accelerator Conference* (JACoW, Melbourne, Australia, 2019), pp. 2625–2628.
- [15] X. Xu, Y. Zhou, and Y. Leng, Machine learning based image processing technology application in bunch longitudinal phase information extraction, *Phys. Rev. Accel. Beams* **23**, 032805 (2020).
- [16] Y. Zhou, Z. Chen, B. Gao, N. Zhang, and Y. Leng, Bunch-by-bunch phase study of the transient state during injection

- tion, *Nucl. Instrum. Methods Phys. Res., Sect. A* **955**, 163273 (2020).
- [17] E. J. Jaeschke, S. Khan, J. R. Schneider, and J. B. Hastings, *Synchrotron Light Sources and Free-Electron Lasers: Accelerator Physics, Instrumentation and Science Applications* (Springer, New York, 2016).
- [18] H. Wiedemann *et al.*, *Particle Accelerator Physics* (Springer, New York, 2007), vol. 314.
- [19] A.-S. Muller, I. Birkel, E. Huttel, F. Perez, M. Pont, and R. Rossmannith, Energy calibration of the anka storage ring, in *Proceedings of the 9th European Particle Accelerator Conference, Lucerne, 2004* (EPS-AG, Lucerne, 2004) [<http://accelconf.web.cern.ch/AccelConf/e04/>].